



HAL
open science

High prevalence of and potential mechanisms for chronic kidney disease in patients with acute intermittent porphyria

Nicolas Pallet, Iadh Mami, Caroline Schmitt, Zoubida Karim, Arnaud François, Marion Rabant, Dominique Nochy, Laurent Gouya, Jean-Charles Deybach, Yichum Xu-Dubois, et al.

► To cite this version:

Nicolas Pallet, Iadh Mami, Caroline Schmitt, Zoubida Karim, Arnaud François, et al.. High prevalence of and potential mechanisms for chronic kidney disease in patients with acute intermittent porphyria. *Kidney International*, 2015, 88 (2), pp.386-395. 10.1038/ki.2015.97 . hal-02317945

HAL Id: hal-02317945

<https://normandie-univ.hal.science/hal-02317945>

Submitted on 16 Oct 2019

HAL is a multi-disciplinary open access archive for the deposit and dissemination of scientific research documents, whether they are published or not. The documents may come from teaching and research institutions in France or abroad, or from public or private research centers.

L'archive ouverte pluridisciplinaire **HAL**, est destinée au dépôt et à la diffusion de documents scientifiques de niveau recherche, publiés ou non, émanant des établissements d'enseignement et de recherche français ou étrangers, des laboratoires publics ou privés.

High prevalence of and potential mechanisms for chronic kidney disease in patients with acute intermittent porphyria

Nicolas Pallet^{1,2,3,4}, Iadh Mami^{1,4}, Caroline Schmitt^{5,6,7}, Zoubida Karim^{6,7}, Arnaud François⁸, Marion Rabant^{4,9}, Dominique Nochy¹⁰, Laurent Gouya^{5,6,7}, Jean-Charles Deybach^{5,6,7}, Yichum Xu-Dubois^{11,12}, Eric Thervet^{3,4}, Hervé Puy^{5,6,7,13} and Alexandre Karras^{3,4,13}

¹INSERM U1147, Centre Universitaire des Saints Pères, Paris, France; ²Service de Biochimie, Hôpital Européen Georges Pompidou, Assistance Publique-Hôpitaux de Paris, Paris, France; ³Service de Néphrologie, Hôpital Européen Georges Pompidou, Assistance Publique-Hôpitaux de Paris, Paris, France; ⁴Université Paris Descartes, Paris, France; ⁵Centre Français des Porphyrines, Hôpital Louis Mourier, Assistance Publique-Hôpitaux de Paris, Colombes, France; ⁶INSERM U1149, Center for Research on Inflammation (CRI), Site Bichat, Paris, France; ⁷Université Paris Diderot, Paris, France; ⁸Service d'Anatomopathologie, Centre Hospitalo-Universitaire Charles Nicolle, Rouen, France; ⁹Service d'Anatomopathologie, Hôpital Necker, Assistance Publique-Hôpitaux de Paris, Paris, France; ¹⁰Service d'Anatomopathologie, Hôpital Européen Georges Pompidou, Assistance Publique-Hôpitaux de Paris, Paris, France; ¹¹INSERM U702, Paris, France and ¹²Université Pierre et Marie Curie, Paris, France

Acute intermittent porphyria (AIP) is a genetic disorder of the synthesis of heme caused by a deficiency in hydroxymethylbilane synthase (HMBS), leading to the overproduction of the porphyrin precursors δ -aminolevulinic acid and porphobilinogen. The aim of this study is to describe the clinical and biological characteristics, the renal pathology, and the cellular mechanisms of chronic kidney disease associated with AIP. A total of 415 patients with HMBS deficiency followed up in the French Porphyria Center were enrolled in 2003 in a population-based study. A follow-up study was conducted in 2013, assessing patients for clinical, biological, and histological parameters. *In vitro* models were used to determine whether porphyrin precursors promote tubular and endothelial cytotoxicity. Chronic kidney disease occurred in up to 59% of the symptomatic AIP patients, with a decline in the glomerular filtration rate of ~ 1 ml/min per 1.73 m² annually. Proteinuria was absent in the vast majority of the cases. The renal pathology was a chronic tubulointerstitial nephropathy, associated with a fibrous intimal hyperplasia and focal cortical atrophy. Our experimental data provide evidence that porphyrin precursors promote endoplasmic reticulum stress, apoptosis, and epithelial phenotypic changes in proximal tubular cells. In conclusion, the diagnosis of chronic kidney disease associated with AIP should be considered in cases of chronic

tubulointerstitial nephropathy and/or focal cortical atrophy with severe proliferative arteriosclerosis.

Kidney International (2015) **88**, 386–395; doi:10.1038/ki.2015.97; published online 1 April 2015

KEYWORDS: cell death; chronic kidney disease; kidney biopsy; renal pathology

Acute intermittent porphyria (AIP) is an inherited autosomal dominant disorder of the synthesis of heme owing to a defect in hydroxymethylbilane synthase (HMBS).^{1,2} The prevalence of symptomatic disease in Europe is 1/180,000,³ but the prevalence of HMBS mutations in the general population is 1/1675,⁴ suggesting that the prevalence of the disease, based on acute AIP symptoms, is underestimated, in part because the clinical manifestations are nonspecific and clinicians are often unaware of the underlying diagnosis. HMBS deficiency fosters the accumulation of the porphyrin precursors δ -aminolevulinic acid (ALA) and porphobilinogen (PBG; Supplementary Figure S1 online). In situations in which heme synthesis is stimulated in the liver, such as during the menstrual cycle, caloric restriction, infection, or the use of medications that induces P450 cytochromes synthesis, the serum concentrations of ALA and PBG greatly increase. This increase may prompt acute symptoms of the disease to occur. The acute clinical expression of AIP is the neurovisceral attack. An AIP acute attack is mainly characterized by severe abdominal pain, often accompanied by nausea, vomiting, tachycardia, and hypertension. The acute attacks may be complicated by neurologic findings: agitation, confusion, peripheral neuropathy, and coma.

During AIP attacks, ALA and PBG are massively excreted in urine, where their presence confirms the diagnosis.⁵ The treatment of AIP relies on the correction/avoidance of precipitating factors, hydration, nutritional support, pain

Correspondence: Nicolas Pallet, Service de Biochimie, Hôpital Européen Georges Pompidou, Assistance Publique-Hôpitaux de Paris, 20, rue Leblanc, Paris 75015, France. E-mail: npallet@yahoo.fr

¹³These authors contributed equally to this work.

Received 12 January 2015; revised 13 February 2015; accepted 19 February 2015; published online 1 April 2015

Table 1 | Clinical and laboratory characteristics of the '2013 cohort' (n = 136)

	AIP patients (n = 74)	Asymptomatic carriers (n = 62)	P-value
Age (years)	65 (56–72)	59 (51–76)	0.3
Time since AIP diagnosis (years)	28 (22–32)	—	—
Chronic AIP (> 4 crisis/year)—n (%)	4 (5.5)	—	—
Female sex—n (%)	62 (87)	41 (68)	0.002
Hypertension—n (%)	46 (62)	25 (42)	0.006
Diabetes—n (%)	2 (3)	3 (5)	0.6
2003 eGFR (ml/min per 1.73 m ²)	60 (48–74)	78 (70–88)	<0.0001
2013 eGFR (ml/min per 1.73 m ²)	51 (41–67)	84 (70–93)	<0.0001
2003 CKD—n (%) ^a	36 (48)	5 (8)	<0.0001
2013 CKD—n (%) ^a	44 (59)	7 (11)	<0.0001
ESRD—n (%) ^b	5 (6.7)	0	<0.0001
Kidney transplantation	2 (2.7)	0	—
Urine protein/creatinine ratio (g/mmol creatinine)	0.04 (0–0.1)	0 (0–0.07)	0.3
Serum uric acid (μmol/l)	372 (316–452)	227 (327–625)	<0.0001
Urine ALA/creatinine (μmol/mmol creatinine) ^c	4 (2.7)	2.6 (1.4–2.6)	<0.0001
Urine PBG/creatinine (μmol/mmol creatinine) ^d	2.1 (4.9–10)	0.4 (0.8–3)	0.007

Abbreviations: AIP, acute intermittent porphyria; ALA, δ-aminolevulinic acid; CKD, chronic kidney disease; eGFR, estimated glomerular filtration rate; ESRD, end-stage renal disease; PBG, porphobilinogen.

Continuous variables are expressed as median and interquartile ranges, and nominal variables as number and proportion. The values are those obtained in 2013, except for those specified as obtained in 2003.

^aCKD is defined as eGFR < 60 ml/min per 1.73 m².

^bESRD was defined as the need for chronic dialysis therapy or kidney transplantation.

^cNormal value < 3 μmol/mmol creatinine.

^dNormal value < 1 μmol/mmol creatinine.

relief, and, in severe cases, administration of heme arginate, which inhibits ALA synthase and reduces ALA and PBG synthesis.⁶ Neurovisceral attacks usually resolve within 4 days.

The long-term complications of AIP include hepatic carcinoma (HCC) without cirrhosis,^{7–9} and chronic kidney disease (CKD). The association of CKD with AIP has been described, and few reports have documented a chronic tubulointerstitial nephropathy with mild hypertension.^{10–13}

No large-scale follow-up study of CKD associated with AIP has been conducted to date, and the biological mechanisms that promote kidney injury are not known. We conducted this population-based, observational study to provide a comprehensive survey of the clinical, biological, and pathological characteristics of CKD associated with AIP (hereafter referred to as PAKD, for porphyria associated kidney disease), and we used *in vitro* models to provide mechanistic insights into how porphyrin precursors might promote kidney injury.

RESULTS

CKD is highly prevalent among AIP patients

In 2003, the French Porphyria Center performed an observational study of a population of 415 patients (184 AIP patients and 231 asymptomatic carriers) who provided a serum creatinine measurement. The demographic characteristics of this population are shown in Supplementary Table S1 online. As expected, most of the patients were lean women, with a median age of 50 years, with a prevalence of liver cancer significantly higher (3%) compared with the asymptomatic carriers (0.4%). Ten years later, in 2013, these 415 patients were contacted by mail to provide responses to a detailed questionnaire and to undergo some specific biological measurements at the steady state of the disease (see

Supplementary Materials and Methods online). The response rate to this survey was 33% (136/415), with 74 AIP patients and 62 asymptomatic carriers (the '2013 cohort'). The demographic and medical characteristics of this cohort are listed in Table 1; except for estimated glomerular filtration rate (eGFR) and age, there was no difference between the 2003 and 2013 cohorts at these two time points. The majority of the AIP patients were female, with no significant difference in age compared with the asymptomatic carriers. As expected, the ALA and PBG urinary concentrations at the steady state were significantly lower in asymptomatic carriers compared with the AIP patients.

CKD, defined as eGFR < 60 ml/min per 1.73 m², was diagnosed in 59% of the AIP patients, compared with 11% in the asymptomatic carriers (Table 1 and Figure 1a). The renal function observed in asymptomatic carriers was similar to the general population.^{14,15} Proteinuria/creatininuria ratio was negligible. Hypertension was frequent in this population, as 62% of the AIP patients were hypertensive, compared with 42% of the asymptomatic carriers ($P = 0.006$). Among the 184 AIP patients in the 2003 cohort, 5 (2.7%) have been identified as having reached end-stage renal disease between 2003 and 2013, and 2 of them received a kidney transplant.

AIP contributes to CKD

Hypertension and 'AIP patients' status occurred more frequently in individuals with CKD (Table 2), and the unadjusted odds ratio for hypertension was 3.8 (95% confidence interval (CI) 1.8–8.1, $P = 0.0004$) and for AIP patients the odds ratio was 11.9 (95% CI 4.6–26, $P < 0.0001$). As AIP patients are frequently hypertensive,¹⁰ and hypertension contributes to CKD, we determined whether AIP was independently associated with CKD (defined by an eGFR < 60

ml/min per 1.73²). The Cochran–Mantel–Haenszel odds ratio adjusted for hypertension was 10.4 (95% CI 3.7–30), with a χ^2 value of 28.2, $P < 0.0001$, indicating that ‘AIP patients’ is an explanatory variable for CKD, independently of hypertension.

The fact that urinary concentrations of PBG were higher in individuals with CKD (Table 2) suggests that urinary

porphyrin precursors could be involved in the pathogenesis PAKD. In line with these findings, the urinary concentrations of neutrophil gelatinase-associated lipocalin, a marker of tubular damage, measured in AIP patients during crisis were higher compared with those in asymptomatic carriers, indicating that acute production of ALA and PBG may promote tubular injury (Supplementary Figure S2 online).

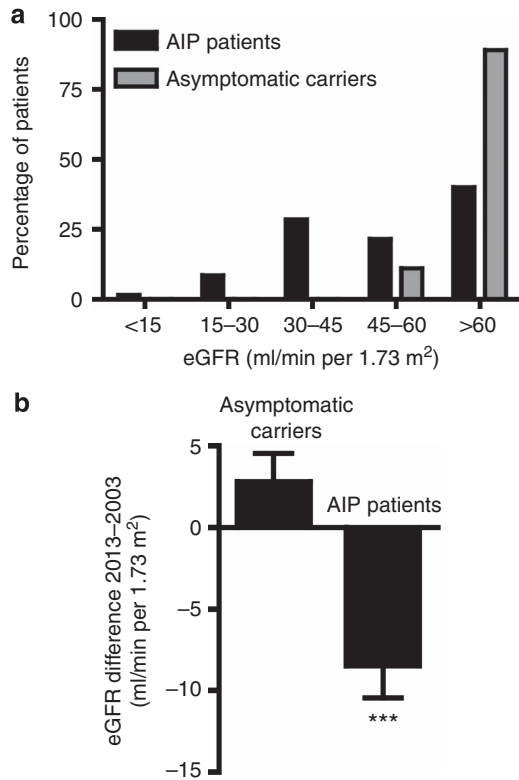


Figure 1 | Characteristics of renal function in acute intermittent porphyria (AIP) patients and asymptomatic carriers. (a) Histogram showing the distribution of the patients according to the 2013 estimated glomerular filtration rate (eGFR) levels in the 2013 cohort. (b) Histogram showing the values of the eGFR variations between 2003 and 2013, according to AIP status (AIP patients or asymptomatic carriers). eGFR is expressed as the mean \pm s.e.m. *** $P < 0.001$ compared with asymptomatic carriers using Student’s *t*-test.

Renal function declines slowly during PAKD

The mean difference of the eGFR between 2013 and 2003 was -8.4 ± 1.9 ml/min per 1.73 m² in the AIP patients, compared with $+1.7 \pm 1.7$ ml/min per 1.73 m² in the asymptomatic carriers ($P < 0.0001$; Figure 1b). We performed a multiple regression analysis to test whether AIP status was independently associated with the decline of renal function between 2003 and 2013 (Delta eGFR). In a model that included potential confounders including age, eGFR at baseline (2003 cohort), and hypertension status, only AIP status and eGFR in 2003 remained significantly correlated with eGFR decline rate (AIP status: estimate -7.5 , 95% CI $(-10.6$ to $-4.3)$; $P < 0.0001$; eGFR in 2003: estimate -0.31 , 95% CI $(-0.47$ to $-0.16)$, $P < 0.0001$), indicating that AIP is an independent risk factor for eGFR degradation over time. Whereas the type of mutation (null allele and missense) was not associated in general with eGFR levels (Table 2) and eGFR decrease between 2003 and 2013 (not shown), we observed that, among AIP patients, the type of mutation could affect eGFR decline rates. For example, AIP patients carrying the c.291delG mutation ($n = 6$; Supplementary Table S2 online) had a eGFR decline of -17.1 ± 3 ml/min per 1.73 m², whereas AIP patients with the c.517C>T missense mutation ($n = 5$) had a eGFR decline of -5 ± 4 ml/min per 1.73 m². There was no difference in terms of urinary ALA or urinary PBG between the two groups of patients. Five out of six (83%) of 291delG-positive patients were hypertensive, compared with two out of five (40%) of 517C>T patients, but this difference did not reach statistical significance ($P = 0.2$, Fisher’s exact test). These results indicate that some specific mutations may be associated with a worse renal prognosis.

Table 2 | Clinical and laboratory characteristics of the ‘2013 cohort’ according the eGFR class

	eGFR < 60 ml/min per 1.73 m ² (n = 54)	eGFR > 60 ml/min per 1.73 m ² (n = 82)	P-value
Age (years)	70 (59–77)	66 (57–74)	0.3
Female sex—n (%)	45 (83)	60 (73)	0.2
Hypertension—n (%)	39 (72)	33 (40)	0.0004
Diabetes—n (%)	2 (3)	3 (3)	1
Body mass index (kg)	23 (21–26)	23 (20–27)	0.79
AIP patients—n (%)	46 (85)	28 (34)	<0.0001
HMBS nonsense mutation—n (%)	31 (57)	44 (53)	0.7
HMBS missense mutation—n (%)	14 (25)	18 (21)	0.4
Urine ALA/creatinine (μ mol/mmol) ^a	2 (3.2–6.7)	2.8 (1.7–6.3)	0.23
Urine PBG/creatinine (μ mol/mmol) ^b	4.4 (1.6–9.7)	1.9 (0.5–6.2)	0.01

Abbreviations: AIP, acute intermittent porphyria; ALA, δ -aminolevulinic acid; eGFR, estimated glomerular filtration rate; PBG, porphobilinogen.

Continuous variables are expressed as median and interquartile ranges and nominal variables as number and proportion.

^aNormal value < 3 μ mol/mmol creatinine.

^bNormal value < 1 μ mol/mmol creatinine.

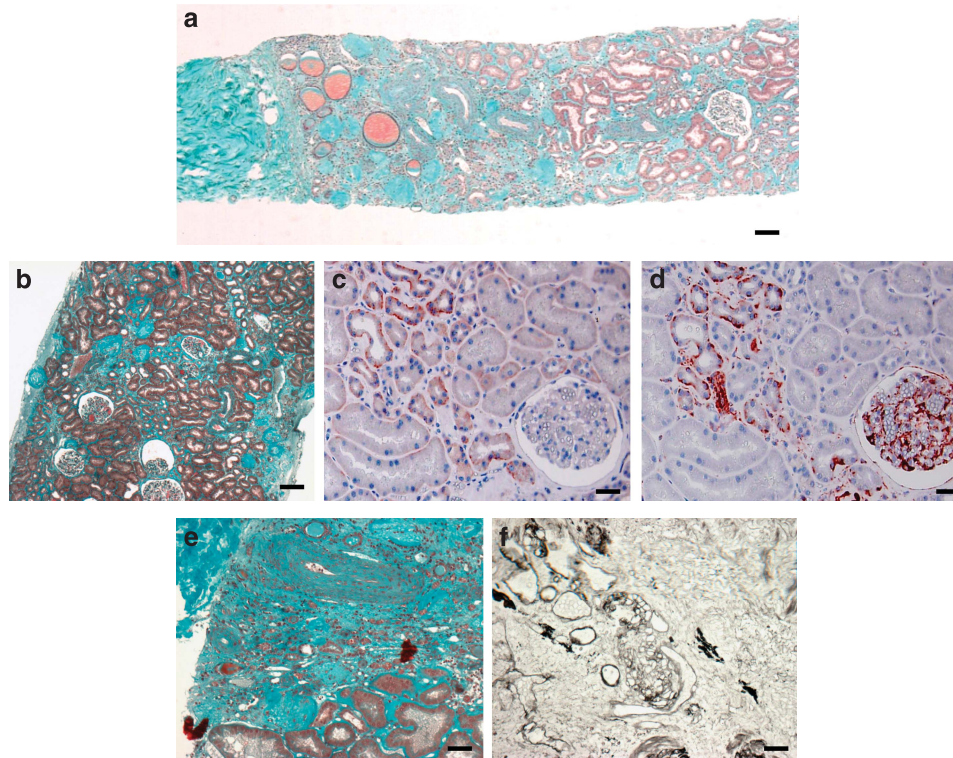


Figure 2 | Renal pathology of porphyria associated kidney disease (PAKD). (a) Percutaneous renal biopsy showing focal cortical atrophy under the renal capsule and numerous sclerotic glomeruli, only one normal glomerulus, arteriosclerosis, and interstitial fibrosis. Masson's trichrome. Bar = 50 μm . (b) Renal biopsy showing vaso-occlusive modifications: interstitial fibrosis with numerous sclerotic glomeruli and numerous ischemic glomeruli with severely retracted tufts. Masson's trichrome. Bar = 50 μm . (c,d) Serial cortical section of a kidney biopsy sample with immunostaining for β -catenin and vimentin. Normal glomeruli are naturally stained by vimentin antibodies, which serve as positive control. Bar = 20 μm . (e) In the superficial cortex under the renal capsule, there was dense interstitial fibrosis with sclerotic glomeruli and vascular lesions of interlobular arteries. Interlobular arteries show cellular and fibrous proliferative intimal thickening with luminal reduction. Masson's trichrome stain. Bar = 50 μm . (f) Intracortical arteriolopathy showing proliferation and swelling of the myocytes of the vascular media (so-called ballooning). Marinuzzi staining (silver staining). Bar = 50 μm .

The tubular epithelium is injured during PAKD

We next reviewed all the available renal biopsies taken from AIP patients included in the 2013 cohort. The histological findings of PAKD in 14 biopsies are summarized in the Supplementary Table S3 online. Except for sclerotic glomeruli, which often represented >50% of the glomeruli in the samples analyzed, and some ischemic glomeruli, no specific glomerular lesions were observed, and no immune deposits were observed when an immunofluorescence analysis was performed (not shown).

Almost all specimens displayed tubular atrophy, basal membrane thickening, and interstitial fibrosis, which were often associated with classical arteriosclerotic lesions of various degrees of severity (Figures 2a and b). Moreover, tubular sections of PAKD biopsies displayed cytoplasmic accumulation of β -catenin and expressed vimentin (Figures 2c and d), indicative of an ongoing fibrogenic process.^{16,17}

Yellow-brown granular aggregates were present both within the proximal tubular cells and in the lumen (Figure 3a), and they were negative for Perl's coloration. The proximal tubules accumulated numerous regular gran-

ular osmiophilic inclusions in their cytoplasm (Figures 3b and c). The size of these particles was 100–500 nm. The other parts of the tubule (distal and collecting tubule) were not affected (Supplementary Figure S3A and B online), and these aggregates were not observed within arterioles (Supplementary Figure S3C online). In addition, ultrastructure analysis of primary cultured human renal epithelial cells (HREC) incubated 72 h with PBG showed accumulation of electron-dense cytosolic granular material (Figure 3d) similar to that observed in renal biopsies.

These data indicate that during AIP proximal tubular cells may accumulate granular components, the composition of which remains undetermined. One possibility is that the polar compound PBG (consisting of one pyrrole ring, Supplementary Figure S1 online) is incorporated within the cells where it is transformed into less soluble uroporphyrinogen I or III (a tetrapyrrole structure), which produces intracellular aggregates. Supporting this, when incubated with proximal tubular cells in culture for 24 h, PBG is totally metabolized into uroporphyrinogen I and III, and cannot be detected in the culture medium (Supplementary Figure S4 online).

Porphyrin precursors promote epithelial injury *in vitro*

We next tested whether ALA and PBG could promote tubular injury by incubating HRECs with 1 mM ALA+PBG, a

concentration that can be reached in AIP patient urine samples upon crisis.¹⁸ When stained with the vital dyes Hoechst 33342 and propidium iodine, HRECs appeared more frequently apoptotic compared with the vehicle-treated cells (Figure 4a). In addition, ALA+PBG induced PARP (polyADP ribose polymerase) cleavage¹⁹ (Figure 4b), and HRECs were more frequently positive for TUNEL (terminal deoxynucleotidyl transferase dUTP nick end labeling) staining (Figure 4c), which confirms that apoptosis is activated in human epithelial cells in culture by ALA+PBG. Mechanistically, ALA and PBG promote eIF2 α phosphorylation and induce the expression of the chaperons BiP/GRP78, PDI, and the apoptosis inducer CHOP (Figures 4d and e), indicating that endoplasmic reticulum stress is activated in HRECs incubated with porphyrin precursors. In addition, HRECs exposed to ALA and PBG accumulated the lipidated form of LC3 (LC3II), indicating that autophagosomes accumulate in these cells, a potential consequence of the activation of the autophagic flux (Figure 4d).

We next tested whether ALA+PBG could induce epithelial phenotypic changes, a process reminiscent of epithelial-to-mesenchymal transition, which is implicated in kidney fibrosis^{17,20} and which is associated with endoplasmic reticulum stress.²⁰ ALA+PBG repressed E-cadherin expression (Figure 4f), and the loss of this epithelial marker was accompanied by a loss of the cuboid morphology of tubular cells, and cell-to-cell contact (Figure 4g). The expression of Slug, a transcription factor that represses E-cadherin expression,²¹ was increased with a nuclear localization (Figure 4g), and β -catenin, which is anchored to E-cadherin in the plasma membrane in resting cells, was translocated in the cytoplasm and the nucleus, where it may regulate mesenchymal programs such as Slug²¹ (Figure 4g). ALA+PBG increased the expression of the profibrotic cytokines epidermal growth factor and transforming growth factor- β , as well as the expression and secretion of the proinflammatory chemokines and cytokines interleukin (IL)-6, monocyte chemotactic protein-1, and IL-8 (Figure 4h and Supplementary Figure S5 online), which indicates that porphyrin precursors may produce a proinflammatory and fibrogenic secretome.

The effects of porphyrin precursors on HREC viability and phenotypic changes appeared to be related to a synergic effect

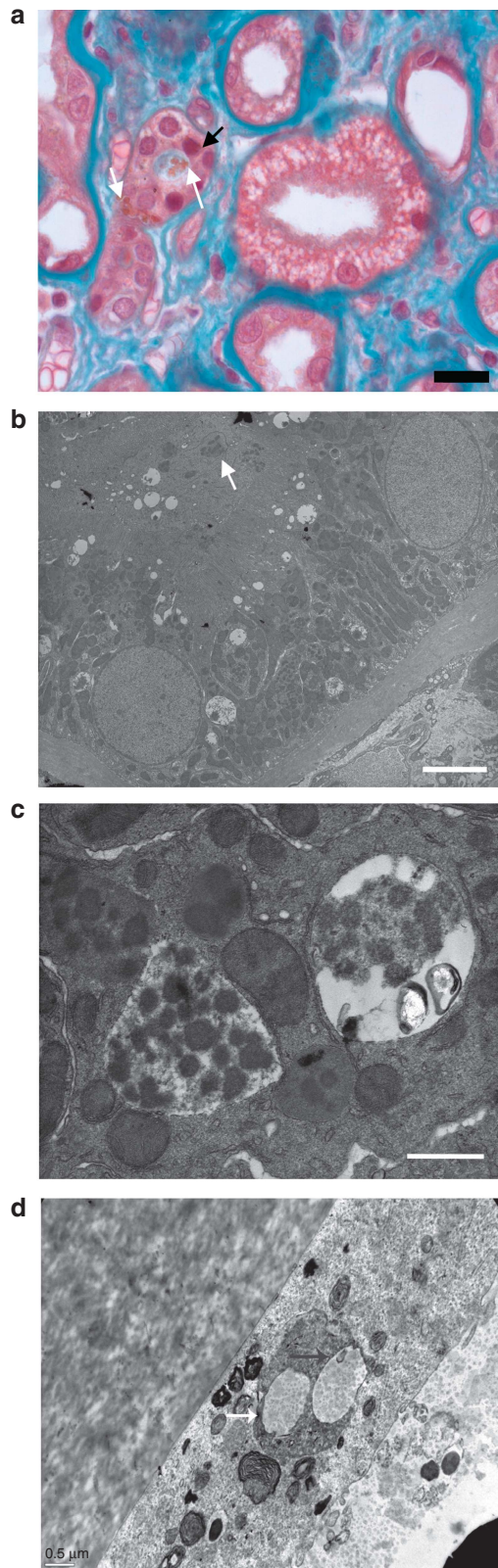


Figure 3 | Tubular accumulation of pigmented granules. (a) Proximal tubule sections with brown aggregates within the cytoplasm and tubule lumen (white arrows). Black arrows denote condensed nuclei, a feature that is suggestive of apoptosis. Bar = 10 μ m. **(b)** Proximal tubule section with basal membrane thickening. Dense osmophilic aggregates are found within the cytoplasm (arrows). Uranyl acetate-lead citrate. Bar = 5 μ m. **(c)** Osmiophilic aggregated granules in the cytoplasm, either embedded in a vesicle or free. Uranyl acetate-lead citrate. Bar = 800 nm. **(d)** Ultrastructure analysis by electron microscopy of human renal epithelial cell in culture incubated for 72 h with porphobilinogen (PBG), showing accumulation of electron-dense cytosolic granular material (white arrows).

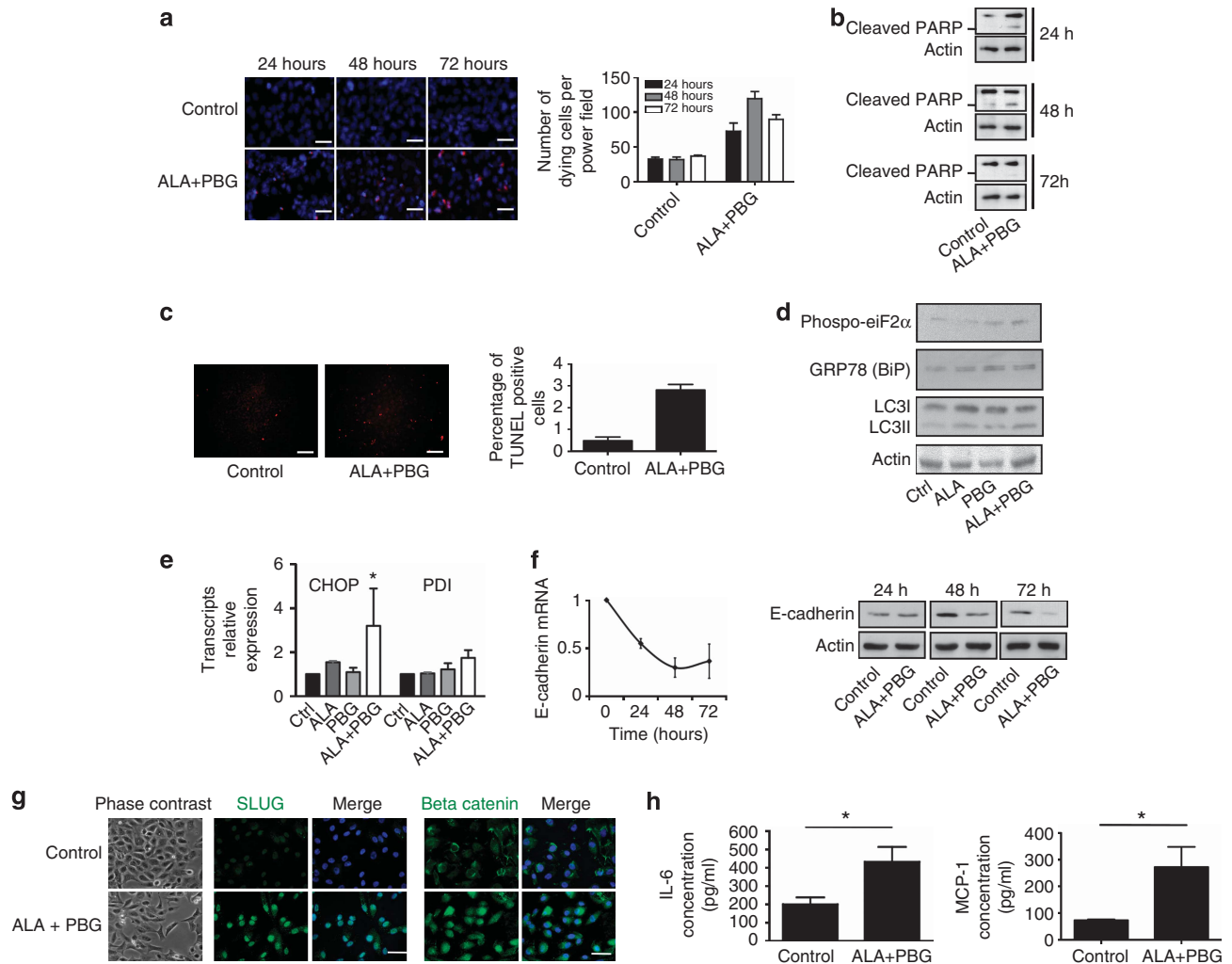


Figure 4 | Porphyrin precursors promote epithelial injury. (a) Human renal epithelial cells (HRECs) were incubated for various periods of time with 1 mM δ -aminolevulinic acid (ALA)+1 mM porphobilinogen (PBG), and then stained with 1 μ g/ml Hoechst 33342 and 5 μ g/ml propidium iodine. The cells were analyzed by fluorescence microscopy. Bar = 50 μ m. An investigator blinded to the experimental conditions estimated the percentages of HO-PI-positive cells adhering to the dishes in three random fields per condition. (b) Immunoblotting for PARP was performed on whole-cell lysates of HRECs that were incubated with 1 mM ALA+1 mM PBG, or maintained in normal medium. Actin is shown as the loading control. Blots are the results of three independent experiments. (c) HRECs were incubated for various periods of time with 1 mM ALA+1 mM PBG, and then stained with TUNEL. Bar = 50 μ m. An investigator blinded to the experimental conditions estimated the percentages of TUNEL-positive cells adhering to the dishes in three random fields per condition. (d) Immunoblotting for phospho-eIF2 α , BiP, and actin was performed on whole-cell lysates of HRECs that were incubated with 1 mM ALA, 1 mM PBG, 1 mM ALA+1 mM PBG, or maintained in normal medium for 24 h. Actin is shown as the loading control. Blots are the results of three independent experiments. (e) Real-time PCR analysis of CHOP and PDI messenger-RNA (mRNA) expression in HRECs after various exposure times to 1 mM ALA, 1 mM PBG, 1 mM ALA+1 mM PBG, or vehicle for 24 h. * $P < 0.05$. (f) Left: real-time PCR analysis of E-cadherin mRNA expression in HRECs after various exposure times to 1 mM ALA+1 mM PBG. Right: representative western blot of E-cadherin expression after various incubation times of 1 mM ALA+1 mM PBG. (g) Left: cellular morphology after 24-h treatment of confluent cells with 1 mM ALA+1 mM PBG or vehicle determined with phase contrast microscopy. Bar = 50 μ m. Middle: immunofluorescence microscopy after slug staining. Bar = 50 μ m. Right: β -catenin nucleocytoplasmic redistribution after 24 h of exposure to vehicle or 1 mM ALA+1 mM. Cells were counterstained with DAPI to demonstrate the nuclei. Bar = 50 μ m. (h) Graph representing the IL-6 and monocyte chemoattractant protein-1 (MCP-1) concentrations (means \pm s.e.m.), measured using enzyme-linked immunosorbent assay (ELISA) using the extracellular medium obtained from a time-course experiment on HRECs incubated with 1 mM ALA and PBG, or vehicle. The data are representative of four independent experiments. TUNEL, terminal deoxynucleotidyl transferase dUTP nick end labeling.

between ALA and PBG because ALA and PBG induced a weak cellular effect on cell death and epithelial phenotypic changes when incubated alone (Supplementary Figure S5 online). In addition, lower concentrations of ALA+PBG (100 μ M) did also promote cell death and phenotypic changes, indicating that porphyrin precursors induce epithelial cell damage even

at low concentrations (Supplementary Figures S5A and S6 online). Taken together, these findings indicate that porphyrin precursors directly promote epithelial cell death and phenotypic changes that may contribute to the pathogenesis of the tubulointerstitial lesions observed during PAKD.

PAKD is associated with severe arteriolar lesions

Severe vascular lesions were observed in 6 out of 14 patients in the absence of antiphospholipid syndrome (Supplementary Table S3 online). The superficial cortex of these kidneys, particularly in the atrophic regions and fibrous areas in which almost all glomeruli were sclerotic (Figure 2a), contained arterial fibrous intimal hyperplasia, characterized by the accumulation of myofibroblasts in the intima and the accumulation of fibrosclerotic tissue, which narrowed the lumen (Figures 2e and f). Given that arterioles are involved in the pathogenesis of PAKD, we tested whether porphyrin precursors could promote endothelial injury: we incubated human endothelial cells (HUVECs) with ALA and PBG and monitored cellular phenotype and viability, and our results indicated that the endothelial cells may not be a direct target for porphyrin precursors (Supplementary Figure S7 online). Therefore, the cellular toxic effects of ALA+PBG appear to be specific for the epithelium.

DISCUSSION

In this study, we have demonstrated that >50% of AIP patients have CKD, and that AIP is an independent risk factor for CKD, even if it is usually associated with hypertension. PAKD progresses slowly and has a mean eGFR decline of ~1 ml/min per 1.73 m² annually. Histopathologically, two types of lesions characterize PAKD: a chronic tubulointerstitial nephropathy, which is often associated with mild and nonspecific arteriosclerosis, and a chronic fibrous intimal hyperplasia associated with focal cortical atrophy. Our results point out a direct role of porphyrin precursors in proximal tubular cell injury, with ALA and PBG promoting epithelial cell death and phenotypic changes that are reminiscent of epithelial-to-mesenchymal transition, with a proinflammatory and a fibrogenic profile.

Inherent to its design, response bias cannot be excluded and may alter the real value of the prevalence of CKD estimated by this study, as the patients who responded could have been more seriously affected by AIP or could have complied better with treatment. However, we report the largest experience of CKD associated with AIP to date, together with the longest follow-up. In 2000, a Swedish population-based study demonstrated for the first time that CKD could be solely owing to AIP.¹⁰ In this cohort, 34 out of 268 AIP patients and asymptomatic carriers had an eGFR <65 ml/min, which is similar to the general population.

The histopathological analyses of kidney biopsies uncover the previously unappreciated importance of the arteriopathy associated with AIP, with severe vascular lesions of fibrous intimal hyperplasia associated with focal cortical atrophy are reminiscent of the primary antiphospholipid syndrome-associated renal vasculopathy.²² This finding raises the question of the potential vascular toxicity of porphyrin precursors, which is highly probable given that ALA promotes vasoconstriction experimentally,^{23,24} that abdominal symptoms are thought to be related, at least in part, to gut ischemia,²⁵ that brain autopsies of AIP patients

who died during crisis indicate the existence of multiple small infarcts,^{26,27} and that AIP attacks may cause posterior reversible encephalopathy.^{28,29}

Our data strongly support a model wherein renal arterioles and tubules are separate targets of porphyrin precursors and that ALA and PBG promote cell epithelial phenotypic changes and apoptosis, leading to a primitive tubulointerstitial nephropathy. It does not exclude the fact that these injuries could be interrelated and that tissue ischemia generated by arterial lumen narrowing could independently fuel tubular atrophy and interstitial fibrosis. An important issue that remains to be resolved is the timing with which renal injuries occur during AIP. We hypothesize that tissue injuries can occur during crisis, when the concentrations of porphyrin precursors peak, and can lead to a cytotoxic effect, followed by injury resolution and subsequent reparation. In this model, the succession of crisis and injury/reparation cycles could progressively generate chronic lesions such as tubular atrophy, interstitial fibrosis, and arteriosclerosis. Arguments supporting this model come from the observation that acute reversible renal failure frequently occurs during AIP crises. The other, but not exclusive, model would favor the chronic toxic effect of slightly elevated concentrations of ALA and PBG, which would lead to slowly evolving lesions. This hypothesis is supported by the fact that the urinary concentration of porphyrin precursors is basally higher for patients, with a lower eGFR compared with patients without kidney dysfunction, in samples taken outside AIP attacks.

Animal models of AIP exist,³⁰ but they do not display obvious renal lesions. In a recent study, Unzu *et al.*³¹ produced acute AIP attacks in *HMBS*-deficient mice by periodically inducing phenobarbital challenge, which caused intermittent accumulation of porphyrin precursors over a period of 3 months. They failed to show any significant impact on renal function and histology, except for small inflammatory infiltrates. It was suggested that the toxic effects of porphyrin precursors on the kidney need extended periods of time to significantly alter renal physiology, as it occurs in the patients who develop PAKD and who are characterized by a relatively constant high excretion of porphyrin precursors throughout years. In line with these results, we did not find significant renal changes, except a slight expansion of the extracellular matrix, even if AIP crisis are triggered with phenobarbital injections for months, or when ALA injections are performed which does not reproduce the pattern of histological lesions encountered in AIP patients (data not shown). It is possible that *HMBS*-deficient mice integrate more complex pathophysiological traits, and may only partly mimic increased urinary concentrations of ALA and PBG. Many factors might explain the fact that *HMBS*-deficient mice do not develop histological lesions similar to those observed in human AIP. The mouse model must retain 30% of *HMBS* activity to be viable. As a consequence, the severity of the renal phenotype is likely reduced. In addition, PAKD progress slowly, and histological lesions take years to become apparent (like lithium nephropathy, for which no animal model exists).

Therefore, the duration of the experiments in HMBS-deficient mice (phenobarbital injections to promote crisis, or ALA injections, during three months) is probably too short to induce significant histological or functional changes that would mimic human PAKD. Finally, the genetic background of HMBS-deficient mice (C57/Bl6) renders them more resistant to kidney injuries compared with other strains, such as FVB/N.³² This may explain, at least in part, the weak renal phenotype observed.

The exact mechanisms by which porphyrin precursors promote cell death remain unclear. DNA damage has been proposed as a trigger for apoptotic cell death.³³ Our findings indicate that ALA and PBG promote endoplasmic reticulum stress and apoptosis. It is tempting to speculate that proximal tubular cells accumulate these compounds after endocytosis, which can spontaneously oligomerize into less soluble uroporphyrinogen, which cannot be degraded, thereby promoting cell stress. Indeed, we have provided in our study ultrastructural and biochemical arguments for an intracellular accumulation of uroporphyrinogen. However, the intracellular disturbances leading to endoplasmic reticulum stress remain to be deciphered. The signaling pathways implicated in chronic tissue injuries during AIP are not known at the molecular level, and whether the long-term kidney disease of AIP shares common pathophysiological mechanisms with extrarenal complications remains to be established. It is noteworthy that in our cohort all patients who suffered from HCC had CKD, suggesting a link between the processes. Epithelial cells incubated with ALA+PBG secrete IL-6. IL-6 is known to foster CKD,^{34–36} and IL-6 has a major role in the development of HCC, as hepatocarcinoma progenitor cells acquire autocrine IL-6 signaling, which stimulates their *in vivo* growth and malignant progression.³⁷ Importantly, this recently described process occurs without preexisting cirrhosis, such as HCC associated with AIP. This may be a general mechanism that drives the chronic complications of AIP and constitutes a potential therapeutic target.

In conclusion, AIP should be considered as one of the possible causes of chronic tubulointerstitial nephritis, or in cases of severe arteriopathy of unknown origin. Physicians should be aware of this association, as HMBS deficiency is frequent, and AIP is probably underdiagnosed, in part because the clinical manifestations are nonspecific and clinicians are often unaware of the underlying diagnosis.

MATERIALS AND METHODS

AIP diagnosis

The criteria for AIP diagnosis followed the European Porphyrin Network guidelines.^{1,38} AIP diagnosis and treatments were performed in the French Porphyrin Center, at the Louis Mourier hospital. The 'AIP patient' status was defined by the association of at least one AIP attack with a typical porphyrin and heme precursors excretion profile in both urine and feces samples; the diagnosis was confirmed by a 50% decrease in HMBS activity in erythrocytes, and complemented by the identification of a causative mutation in HMBS gene by direct sequencing, as previously described.³⁹ Urinary

ALA and PBG were measured using the Bio-Rad ALA/PBG column kit (Hercules, CA), according to the manufacturer's protocol.

The 'asymptomatic carrier' status is defined after a family screening to identify those with latent disease, and it is based on a deficient HMBS enzymatic activity complemented with a DNA analysis by direct sequencing to identify the causative mutation in the HMBS gene (which requires prior identification of the mutation in a related affected family member).

Study population

In 2003, a nationwide observational study surveyed a population of 415 patients (184 AIP patients and 231 asymptomatic carriers), who provided a serum creatinine measurement. In 2013, these patients were contacted by mail to provide detailed information including AIP symptoms, presence of hypertension, or diabetes. Biological analysis included serum creatinine, eGFR evaluation using the 4-variable MDRD formula, ALA and PBG urinary concentrations, and measurements of the protein-to-creatinine ratio in a morning urine sample. The institutional review board of Louis Mourier Hospital approved the study, written informed consent was obtained from all patients, and the database has been deposited to the Commission Nationale Informatique et Libertés (CNIL, agreement number 1187326).

Histology, electron microscopy, and immunochemistry

All the available renal biopsies taken from AIP patients included in the 2013 cohort were retrospectively analyzed. Examinations of the specimens were performed using standard Masson's staining, Marinuzzi's silver stain, Perls coloration, and ultrastructural analysis by electron microscopy. Immunohistochemistry for vimentin and beta catenin was performed on the paraffin-embedded tissues as described previously.¹⁷ For more details, see the 'Extended Methods' section in the Supplementary Appendix online.

Cell culture

HRECs were retrieved from human nephrectomy specimens and isolated according to previously published methods, with minor modifications^{40,41} (see the 'Extended Methods' section in the Supplementary Appendix online). The concentration of ALA and PBG used to incubate cells was 1 mmol/l to mimic the urinary concentrations of ALA and PBG found during the AIP attacks.

Immunoblotting

Total protein lysates from HRECs were separated by SDS polyacrylamide gel electrophoresis under denaturing conditions and transferred to a PVDF membrane (GE Healthcare, Vélizy-Villacoublay, France). Primary antibodies were visualized using horseradish peroxidase-conjugated polyclonal secondary antibodies (Dako, Glostrup, Denmark) and detected using ECL reagent (GE Healthcare). See the 'Extended Methods' section in the Supplementary Appendix online.

Quantitative polymerase chain reaction

Transcript expression levels were measured by SYBR green qPCR using an ABI PRISM 7900 sequence detector system (Applied Biosystems, Fontenay-sous-Bois, France). Vehicle-treated samples were used as controls, and fold changes for each tested gene were normalized to the Ribosomal Protein L13A (*RPL13A*) housekeeping gene. The relative expression levels were calculated using the $2^{-\Delta\Delta CT}$ method.⁴² For more details including the sequences of the

primers, see the ‘Extended Methods’ section in the Supplementary Appendix online.

Terminal deoxynucleotidyl transferase dUTP nick end labeling (TUNEL)

TUNEL staining was performed with the In Situ Cell Death Detection Kit, Fluorescein (Roche, Meylan, France), according to the manufacturer’s instructions. Samples were counterstained with DAPI to visualize nuclei. The number of TUNEL positive nuclei per high power field was reported to the number of DAPI positive nuclei to calculate the percentage of TUNEL positive nuclei on at least 4 fields (×100) per sample.

Fluorescence microscopy

Epifluorescence microscopy was performed on HRECs, which were stained with Hoechst 33342 (2’-(4-ethoxyphenyl)-5-(4-methyl-1-piperazinyl)-2,5’-bi-1H-benzimidazole) (Sigma Aldrich, St Louis, MO) and propidium iodide (Invitrogen, Fontenay-sous-Bois, France), as previously described.⁴³ Indirect immunofluorescence to detect slug and beta-catenin was performed using confocal microscopy (see the ‘Extended Methods’ section in the Supplementary Appendix online).

Enzyme-linked immunosorbent assay

The secretion of IL-6 and monocyte chemotactic protein-1 was measured in the cell culture supernatant using the Quantikine human IL6 and monocyte chemotactic protein-1 immunoassays (R&D Systems, Minneapolis, MN) according to the manufacturer’s protocol. neutrophil gelatinase-associated lipocalin concentrations in urine samples was measured using the Quantikine human neutrophil gelatinase-associated lipocalin immunoassay, according to the manufacturer’s protocol.

Statistical analysis

The results for the categorical variables were expressed as frequencies and percentages and for the continuous variables as the mean ± s.e.m. Associations between the clinical and biological features of the patients were tested using Student’s *t*-test or the χ^2 test where appropriate. All tests were two sided, and a *P*-value < 0.05 was considered statistically significant. Stratified odds ratio and χ^2 were obtained using the Cochran–Mantel–Haenszel test. The statistical analyses were performed using the R framework (available from: <http://www.R-project.org/>).

DISCLOSURE

All the authors declared no competing interests.

ACKNOWLEDGMENTS

We thank Dany Anglicheau for providing MCP-1 ELISA.

SUPPLEMENTARY MATERIAL

Figure S1. Porphyrin metabolism and heme synthesis.

Figure S2. Urinary neutrophil gelatinase associated lipocalin concentrations during AIP crisis.

Figure S3. Ultrastructure of tubules and arterioles.

Figure S4. Concentrations of PBG and uroporphyrinogen in HREC and culture medium.

Figure S5. HREC incubated with ALA and PBG alone.

Figure S6. Effects of low concentrations of porphyrin precursors on HREC.

Figure S7. Effect of porphyrin precursors on HUVEC.

Table S1. Characteristics of the 2003 cohort.

Table S2. Characteristics of the HMBS mutations in the 2013 cohort.

Table S3. Histopathology of PAKD.

Supplementary material is linked to the online version of the paper at <http://www.nature.com/ki>

REFERENCES

1. Puy H, Gouya L, Deybach JC. Porphyrrias. *Lancet* 2010; **375**: 924–937.
2. Siegesmund M, van Tuyl van Serooskerken AM, Poblete-Gutierrez P et al. The acute hepatic porphyrias: current status and future challenges. *Best Pract Res Clin Gastroenterol* 2010; **24**: 593–605.
3. Elder G, Harper P, Badminton M et al. The incidence of inherited porphyrias in Europe. *J Inherit Metab Dis* 2013; **36**: 849–857.
4. Nordmann Y, Puy H, Da Silva V et al. Acute intermittent porphyria: prevalence of mutations in the porphobilinogen deaminase gene in blood donors in France. *J Intern Med* 1997; **242**: 213–217.
5. Herrick AL, McColl KE. Acute intermittent porphyria. *Best Pract Res Clin Gastroenterol* 2005; **19**: 235–249.
6. Anderson KE, Bloomer JR, Bonkovsky HL et al. Recommendations for the diagnosis and treatment of the acute porphyrias. *Ann Intern Med* 2005; **142**: 439–450.
7. Andant C, Puy H, Bogard C et al. Hepatocellular carcinoma in patients with acute hepatic porphyria: frequency of occurrence and related factors. *J Hepatol* 2000; **32**: 933–939.
8. Andant C, Puy H, Faivre J et al. Acute hepatic porphyrias and primary liver cancer. *N Engl J Med* 1998; **338**: 1853–1854.
9. Stewart MF. Review of hepatocellular cancer, hypertension and renal impairment as late complications of acute porphyria and recommendations for patient follow-up. *J Clin Pathol* 2012; **65**: 976–980.
10. Andersson C, Wikberg A, Stegmayr B et al. Renal symptomatology in patients with acute intermittent porphyria. A population-based study. *J Intern Med* 2000; **248**: 319–325.
11. Marsden JT, Chowdhury P, Wang J et al. Acute intermittent porphyria and chronic renal failure. *Clin Nephrol* 2008; **69**: 339–346.
12. Andersson C, Lithner F. Hypertension and renal disease in patients with acute intermittent porphyria. *J Intern Med* 1994; **236**: 169–175.
13. Sardh E, Andersson DE, Henrichson A et al. Porphyrin precursors and porphyrins in three patients with acute intermittent porphyria and end-stage renal disease under different therapy regimes. *Cell Mol Biol* 2009; **55**: 66–71.
14. Castro AF, Coresh J. CKD surveillance using laboratory data from the population-based National Health and Nutrition Examination Survey (NHANES). *Am J Kidney Dis* 2009; **53**: S46–S55.
15. Rule AD, Gussak HM, Pond GR et al. Measured and estimated GFR in healthy potential kidney donors. *Am J Kidney Dis* 2004; **43**: 112–119.
16. Hazzan M, Hertig A, Buob D et al. Epithelial-to-mesenchymal transition predicts cyclosporine nephrotoxicity in renal transplant recipients. *J Am Soc Nephrol* 2011; **22**: 1375–1381.
17. Hertig A, Anglicheau D, Verine J et al. Early epithelial phenotypic changes predict graft fibrosis. *J Am Soc Nephrol* 2008; **19**: 1584–1591.
18. Marsden JT, Rees DC. Urinary excretion of porphyrins, porphobilinogen and delta-aminolaevulinic acid following an attack of acute intermittent porphyria. *J Clin Pathol* 2014; **67**: 60–65.
19. Kepp O, Galluzzi L, Lipinski M et al. Cell death assays for drug discovery. *Nat Rev Drug Discov* 2011; **10**: 221–237.
20. Pallet N, Bouvier N, Bendjallah A et al. Cyclosporine-induced endoplasmic reticulum stress triggers tubular phenotypic changes and death. *Am J Transplant* 2008; **8**: 2283–2296.
21. Thiery JP, Sleeman JP. Complex networks orchestrate epithelial-mesenchymal transitions. *Nat Rev Mol Cell Biol* 2006; **7**: 131–142.
22. Nochy D, Daugas E, Droz D et al. The intrarenal vascular lesions associated with primary antiphospholipid syndrome. *J Am Soc Nephrol* 1999; **10**: 507–518.
23. Chang CJ, Lee YH, Yang JY et al. Pilot *in vitro* toxicity study of 5-ALA and Photofrin in microvascular endothelial cell cultures. *J Clin Laser Med Surg* 1997; **15**: 83–87.
24. Middelburg TA, de Bruijn HS, Tettero L et al. Topical hexylaminolevulinat and aminolevulinic acid photodynamic therapy: complete arteriole vasoconstriction occurs frequently and depends on protoporphyrin IX concentration in vessel wall. *J Photochem Photobiol B* 2013; **126**: 26–32.
25. Lithner F. Could attacks of abdominal pain in cases of acute intermittent porphyria be due to intestinal angina? *J Intern Med* 2000; **247**: 407–409.
26. Kupferschmidt H, Bont A, Schnorf H et al. Transient cortical blindness and bioccipital brain lesions in two patients with acute intermittent porphyria. *Ann Intern Med* 1995; **123**: 598–600.

27. Lai CW, Hung TP, Lin WS. Blindness of cerebral origin in acute intermittent porphyria. Report of a case and postmortem examination. *Arch Neurol* 1977; **34**: 310–312.
28. Celik M, Forta H, Dalkilic T et al. MRI reveals reversible lesions resembling posterior reversible encephalopathy in porphyria. *Neuroradiology* 2002; **44**: 839–841.
29. Soysal A, Dogan P, Dayan C et al. Reversible MRI findings of porphyric encephalopathy. A report of two cases. *Neuroradiol J* 2008; **21**: 655–659.
30. Lindberg RL, Porcher C, Grandchamp B et al. Porphobilinogen deaminase deficiency in mice causes a neuropathy resembling that of human hepatic porphyria. *Nat Genet* 1996; **12**: 195–199.
31. Unzu C, Sampedro A, Sardh E et al. Renal failure affects the enzymatic activities of the three first steps in hepatic heme biosynthesis in the acute intermittent porphyria mouse. *PLoS One* 2012; **7**: e32978.
32. Viau A, El Karoui K, Laouari D et al. Lipocalin 2 is essential for chronic kidney disease progression in mice and humans. *J Clin Invest* 2010; **120**: 4065–4076.
33. De Siervi A, Vazquez ES, Rezaval C et al. Delta-aminolevulinic acid cytotoxic effects on human hepatocarcinoma cell lines. *BMC Cancer* 2002; **2**: 6.
34. Zhang XL, Topley N, Ito T et al. Interleukin-6 regulation of transforming growth factor (TGF)-beta receptor compartmentalization and turnover enhances TGF-beta1 signaling. *J Biol Chem* 2005; **280**: 12239–12245.
35. Dai Y, Zhang W, Wen J et al. A2B adenosine receptor-mediated induction of IL-6 promotes CKD. *J Am Soc Nephrol* 2011; **22**: 890–901.
36. Zhang W, Wang W, Yu H et al. Interleukin 6 underlies angiotensin II-induced hypertension and chronic renal damage. *Hypertension* 2012; **59**: 136–144.
37. He G, Dhar D, Nakagawa H et al. Identification of liver cancer progenitors whose malignant progression depends on autocrine IL-6 signaling. *Cell* 2013; **155**: 384–396.
38. Tollanes MC, Aarsand AK, Villanger JH et al. Establishing a network of specialist Porphyria centres - effects on diagnostic activities and services. *Orphanet J Rare Dis* 2012; **7**: 93.
39. Puy H, Deybach JC, Lamoril J et al. Molecular epidemiology and diagnosis of PBG deaminase gene defects in acute intermittent porphyria. *Am J Hum Genet* 1997; **60**: 1373–1383.
40. Tang S, Leung JC, Abe K et al. Albumin stimulates interleukin-8 expression in proximal tubular epithelial cells *in vitro* and *in vivo*. *J Clin Invest* 2003; **111**: 515–527.
41. Pallet N, Thervet E, Le Corre D et al. Rapamycin inhibits human renal epithelial cell proliferation: effect on cyclin D3 mRNA expression and stability. *Kidney Int* 2005; **67**: 2422–2433.
42. Livak KJ, Schmittgen TD. Analysis of relative gene expression data using real-time quantitative PCR and the 2(-Delta Delta C(T)) Method. *Methods* 2001; **25**: 402–408.
43. Sirois I, Groleau J, Pallet N et al. Caspase activation regulates the extracellular export of autophagic vacuoles. *Autophagy* 2012; **8**: 927–937.